

***s*-wave superconductivity probed by measuring magnetic penetration depth and lower critical field of MgCNi₃ single crystals**

P. Diener,¹ P. Rodière,¹ T. Klein,^{1,2} C. Marcenat,^{3,4} J. Kacmarcik,⁴ Z. Pribulova,⁴ D. J. Jang,⁵ H. S. Lee,⁵ H. G. Lee,⁶ and S. I. Lee⁶

¹*Institut Néel, CNRS/UJF, 25 Rue des Martyrs, BP 166, 38042 Grenoble Cedex 9, France*

²*Institut Universitaire de France and Université Joseph Fourier, BP 53, 38041 Grenoble Cedex 9, France*

³*CEA, Institut Nanosciences et Cryogénie, SPSMS-LATEQS, 17 Rue des Martyrs, 38054 Grenoble Cedex 9, France*

⁴*Slovak Academy Sciences, Institut of Experimental Physics, Center for Low Temperature Physics, Safarik University, Kosice 04001, Slovakia*

⁵*Department of Physics, Pohang University of Science and Technology, Pohang 790-784, Republic of Korea*

⁶*Department of Physics, National Creative Research Initiative Center for Superconductivity, Sogang University, Seoul 100-611, Republic of Korea*

(Received 29 April 2009; published 18 June 2009)

The magnetic penetration depth λ has been measured in MgCNi₃ single crystals using both a high-precision tunnel diode oscillator (TDO) technique and Hall probe magnetization (HPM). In striking contrast to previous measurements in powders, $\delta\lambda(T)$ deduced from TDO measurements increases exponentially at low temperature, clearly showing that the superconducting gap is fully open over the whole Fermi surface. An absolute value at zero temperature $\lambda(0)=230$ nm is found from the lower critical field measured by HPM. We also discuss the observed difference of the superfluid density deduced from both techniques. A possible explanation could be due to a systematic decrease in the critical temperature at the sample surface.

DOI: [10.1103/PhysRevB.79.220508](https://doi.org/10.1103/PhysRevB.79.220508)

PACS number(s): 74.25.Nf, 74.25.Op, 74.70.Dd

The interplay between magnetism and superconductivity is currently a subject of great interest. In the UGe₂ and URhGe uranium compounds, for instance, a long-range ferromagnetic ordered phase coexists with the superconducting phase and a mechanism of spin fluctuations (SFs) could be at the origin of the Cooper pair formation.^{1,2} The recent discovery of high-temperature superconductivity in oxypnictides also rapidly became the topic of a tremendous number of both experimental and theoretical works. The parent undoped LnOFeAs (where Ln=La, Sm, ...) compound is here close to itinerant magnetism due to the presence of a high density of Fe *d* states at the Fermi level,³ leading to competing ferromagnetic and antiferromagnetic fluctuations. Similarly in the cubic (anti)perovskite MgCNi₃ compound,⁴ the presence of a strong Van Hove singularity in the density of Ni states slightly below the Fermi level also leads to strong ferromagnetic fluctuations.⁵⁻⁹ These two systems have also a Fermi surface composed of both electron and hole pockets three-dimensional (3D) (sheets in MgCNi₃ as compared to quasi-cylindrical sheets in oxypnictides).

Despite these striking similarities in their electronic and magnetic properties, spin fluctuations lead to very different effects in those systems. On the one hand, *ab initio* calculations rapidly showed that the electron-phonon coupling constant ($\lambda_{e-ph} \sim 0.2$) is far too low to account for the high critical temperatures observed in oxypnictides (up to ~ 55 K) and an unconventional mechanism mediated by the SF associated with a sign reversal of the (*s*-wave) order parameter between electron and hole sheets of the Fermi surface has been proposed.¹⁰ On the other hand, it has been suggested that the narrow Van Hove singularity could be responsible for a nearly unstable phonon mode in MgCNi₃ inducing a large, although reduced by SF, λ_{e-ph} ,^{11,12} in agreement with experiments which yield an average electron-phonon coupling constant in the order of 1.7.^{11,13,14} The interplay be-

tween electron-phonon coupling and SF is further emphasized in this system by the existence of a large isotopic effect¹⁵ which has been suggested to be enhanced by the strong SF.¹⁶

In this context, the nature of the superconducting order parameter rapidly became a crucial issue. In MgCNi₃, the experimental results still remain controversial: on the one hand, penetration depth measurements (in polycrystalline samples) showed a quadratic, i.e., non-*s*-wave, temperature dependence suggesting a nodal order parameter,¹⁷ whereas specific-heat measurements clearly indicate that the superconducting gap (Δ) is fully open, with a $\Delta/k_B T_c$ ratio ranging from 1.9 to 2.1,^{13,18,19} i.e., well above the BCS weak-coupling 1.76 value.

In this Rapid Communication, we present high-precision magnetic penetration depth and lower critical field measurements performed in the same MgCNi₃ single crystals. We show that $\lambda(T)$ clearly follows an exponential temperature dependence for $T < T_c/3$ showing that the gap is fully open over the whole Fermi surface. A zero temperature λ_0 value of 230 nm, i.e., well above the London clean limit BCS value (~ 60 nm) has been deduced from first penetration field measurements, clearly suggesting the presence of strong mass renormalization and/or impurity scattering effects. Introducing this value into the tunnel diode oscillator (TDO) data however leads to a temperature dependence of the normalized superfluid density $\frac{\rho_s(T)}{\rho_s(0)} = \left[\frac{1}{1 + \delta\lambda(T)/\lambda_0} \right]^2$ which is different from the one directly deduced from the lower critical field [$H_{c1} \propto \ln(\kappa)/\lambda^2$, where $\kappa = \lambda/\xi$]. Possible reasons for this discrepancy are discussed.

Single crystals were grown in a high-pressure furnace as described elsewhere.²⁰ Ac specific heat have been performed on several samples of the same batch.²¹ All the measured crystals show sharp superconducting transitions ($\Delta T_c \sim 0.2$ K) emphasizing the excellent bulk homogeneity of

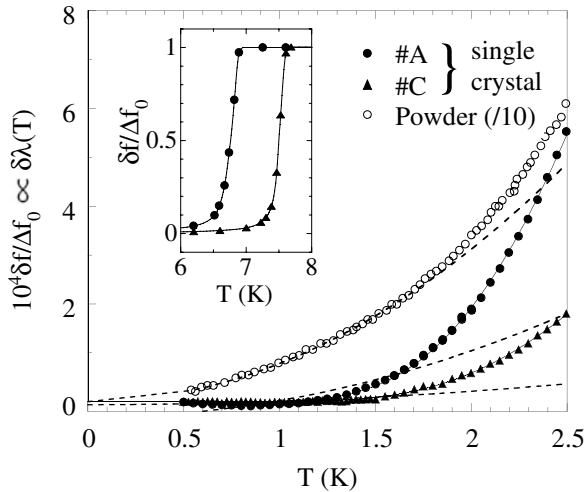


FIG. 1. Low-temperature TDO frequency shift δf normalized by the frequency shift for a total extraction obtained for single crystals A and C. Open circles correspond to previous results on polycrystalline powders (Ref. 17) divided by a factor 10. The dashed line is the T^2 law below 1.8 K reported for the powder. In the case of the single crystals, a better fit is obtained with an exponential law (solid line). Inset: frequency shift at the critical temperature for both single crystals.

each crystal. We observed however a large dispersion of critical temperatures from sample to sample, between approximately 5.9–7.6 K, probably due to a slight Ni deficiency in the MgCNi_3 structure.²⁰ Three single crystals with a thickness of 0.1 mm but different shapes and critical temperatures have been selected. Sample A can be approximated by a disk with a diameter of 0.3 mm. Samples B and C have a rectangular shape of 0.21×0.15 and 0.24×0.36 mm², respectively. Samples A and B both present a bulk T_c of 6.9 K and exhibit exactly the same behavior by TDO and Hall probe magnetization (HPM), whereas sample C has the highest T_c at 7.6 K.

The magnetic penetration depth has been measured with a high stability LC oscillator operating at 14 MHz driven by a tunnel diode.^{22,23} The ac excitation field is below 1 μT and the dc earth magnetic field is screened by a demagnetized weak ferromagnet amorphous ribbon ensured to work well below H_{c1} . The sample stage placed at the bottom of a homemade He^3 refrigerator is regulated between 0.5 and 10 K, whereas the LC oscillator remains at fixed temperature. The superconducting sample is glued with vacuum grease at the bottom of a sapphire cold finger, which can be extracted *in situ*.²⁴ The small filling factor of the excitation coil by the superconducting sample ($\sim 0.01\%$) ensures a small perturbation of the circuit, and the frequency shift δf divided by the one induced by the extraction of the superconducting sample, Δf_0 , is then proportional to the imaginary part of the surface impedance and hence to the magnetic penetration depth.²⁵ As shown in the inset of Fig. 1, all samples present a sharp superconducting transition at a critical temperature T_c^f (defined by the onset of the frequency shift change) equal to 6.9 K (respectively, 7.6 K) for sample A (respectively, sample C) in good agreement with the C_p measurements.

Figure 1 displays the temperature dependence of the fre-

quency shift, proportional to $\delta\lambda(T)$, compared to the results previously reported in powders.¹⁷ The amplitude of the shift is ten times larger in the case of the powder reflecting the fact that the surface on which the supercurrents are flowing is much larger in powders than in single crystals (for the same sample volume). It is important to note that the temperature dependence of λ is strikingly different in single crystals than in powder for which a T^2 power law has been reported below 1.8 K. Such a dependence has been interpreted as an evidence for unconventional superconductivity,¹⁷ but our measurements do not support this scenario as a T^2 power law only very poorly describes the experimental data (see dashed line in Fig. 1).

A very good fit to our data is actually obtained assuming the low-temperature approximation for clean type II superconductors with a fully open gap: $\lambda(T) \propto \sqrt{\Delta/k_B T} e^{-\Delta/k_B T}$. This expression is valid for $k_B T < \Delta/5$ and leads to $\Delta/k_B = 11.6(1)$ K for sample A (and B) and $\Delta/k_B = 12.3(1)$ K for sample C. Note that this fitting procedure can lead to a slightly overestimated Δ value (up to 10%, depending on the range of the fit and the ratio between Δ and T_c) but unambiguously shows that the gap is fully open in good agreement with previous tunneling spectroscopy,^{26,27} NMR,⁸ and specific-heat measurements which led to $\Delta/k_B \approx 13.0(2)$, 10.5, and 13 K, respectively.

However, fitting the low-temperature data only leads to the size of the minimum superconducting gap. To unambiguously exclude the presence of any other gaps (and/or other gap symmetries) it is necessary to analyze the full temperature dependence of the normalized superfluid density $\rho_S(T) \propto 1/\lambda(T)^2$ up to T_c . This superfluid density can be deduced as follows:

(i) either from the temperature dependence of the lower critical field: $H_{c1} = \Phi_0^2 / (4\pi\lambda^2) [Ln(\kappa) + c(\kappa)]$, where $\kappa = \lambda/\xi$ (ξ being the coherence length) and $c(\kappa)$ is a κ dependent function tending toward ~ 0.5 for large κ values. As κ is almost temperature independent (being in the order of 40), $H_{c1}(T)$ is directly proportional to the superfluid density which we will call ρ_S^{Hc1} .

(ii) or by introducing the absolute value of the penetration depth at $T=0$ K (λ_0) into the TDO data: $\rho_S^{\text{TDO}}(T) \propto \left[\frac{1}{1 + \delta\lambda(T)/\lambda_0} \right]^2 = \left[\frac{1}{1 + \delta f(T)/\Delta f_0 \times R/\lambda_0} \right]^2$, where R is a geometrical factor.²⁸

The local magnetic induction has been measured with a miniature 16×16 μm^2 Hall probe and the first penetration field H_p has been deduced by measuring the remanent field (B_{rem}) in the sample after applying an external field H_a and sweeping the field back to zero. For $H_a < H_p$ (i.e., in the Meissner state) no vortices penetrate the sample and the remanent field remains equal to zero (actually close to zero due to partial penetration through the sample corners). H_a is then progressively increased until a finite remanent field is obtained (see Fig. 2). Indeed, since vortices remain pinned in the sample, B_{rem} rapidly increases for $H_a > H_p$, varying as $(H_a - H_p)^\alpha$ with $\alpha = 0.4 \pm 0.1$ (solid lines in Fig. 2 for $\alpha = 0.5$). We get $H_p \sim 50 \pm 5$, $\sim 55 \pm 5$ and $\sim 70 \pm 10$ G for samples A, B and C, respectively. In samples with rectangular cross sections, H_p is then related to H_{c1} through $H_{c1} \approx H_p / \tanh(\sqrt{ad}/2w)$, where α varies from 0.36 in strips to

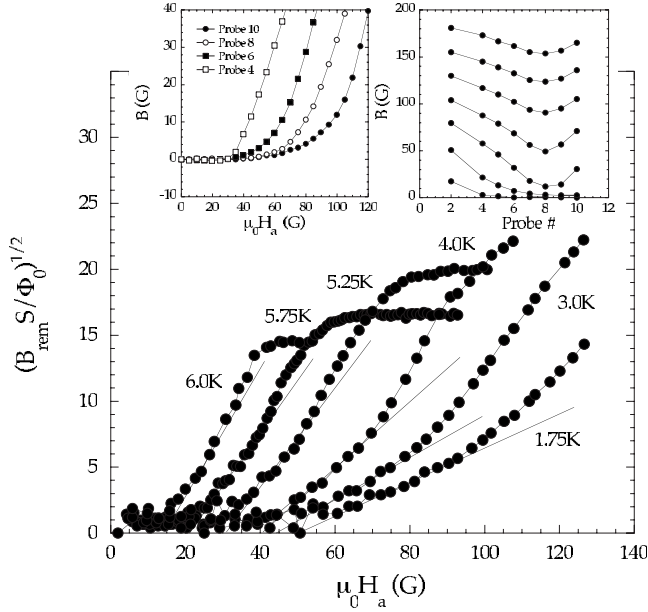


FIG. 2. Remanent field B_{rem} in flux quantum units (Φ_0/S , with S being the active area of the probe) as a function of the applied field H_a in sample A showing that B_{rem} remains close to zero up to $H_a = H_p$ (see text for details). Left inset: local induction at $T=4.2$ K as a function of the applied field for several probe positions (see right inset) showing that, even the penetration is much stronger close to the edges (probe 4), the same first penetration field (~ 35 G) can be obtained on all of the probes. Right inset: field profiles at $T=4.2$ K for different values of the applied field (measured on probe 2) clearly showing the Bean profile characteristic of bulk pinning. Probe 8 is located close to the center of the sample and probe 4 close to the sample edge. The spacing between probes is $20 \mu\text{m}$.

0.67 in disks.^{29,30} Taking an average α value ~ 0.5 we hence get $H_{c1}^c(0) \sim 125 \pm 15$ G and correspondingly $\lambda_0 = 230 \pm 15$ nm [introducing $H_{c2}(0) = \Phi_0 / 2\pi\xi(0)^2 = 9.5$ T (Ref. 21)].

This value is in good agreement with the value deduced from muon spin relaxation data in ceramics,³¹ previous lower critical field measurements in powder³² as well as the value calculated from the thermodynamic critical field deduced from specific-heat measurements by Wälte *et al.*

Note that, as pointed out by Wälte *et al.*, this value is much larger than the London clean limit BCS value $\lambda_L(0) = c/\omega_p \sim 60$ nm [ω_p being the plasma frequency ~ 3.2 eV (Ref. 13)]. In the presence of strong mass renormalization and/or impurity scattering effects $\lambda_0 = \lambda_L(0) \sqrt{1 + \lambda_{e\text{-ph}}} \sqrt{1 + \xi_0/l}$, where l is the mean free path and $\xi_0 \sim \frac{\hbar v_F}{\pi \Delta_0}$ (v_F being the bare Fermi velocity). Introducing $\lambda_{e\text{-ph}} \sim 1.8$ and $v_F \sim 2.1 \times 10^5$ m s⁻¹,¹³ one obtains $l \sim \xi_0/4 \sim 10$ nm and hence confirms that both strong coupling and strong impurity diffusion are present. Note that this l value corresponds to a resistivity $\rho = v_F / \epsilon_0 l \omega_p^2 \sim 10 \mu\Omega$ cm, i.e., slightly lower than the residual resistivity measured in similar crystals $\rho \sim 30 \mu\Omega$ cm.²⁰ However, since ρ is expected to be in the order of $\lambda_0^2 \mu_0 \pi \Delta / \hbar (1 + \lambda_{e\text{-ph}})$ (dirty limit), a residual resistivity of $30 \mu\Omega$ cm value would thus require that $\lambda_{e\text{-ph}} \ll 1$ in striking contrast with reported values.

ρ_S^{Hc1} (solid symbols) and ρ_S^{TDO} (open symbols) are dis-

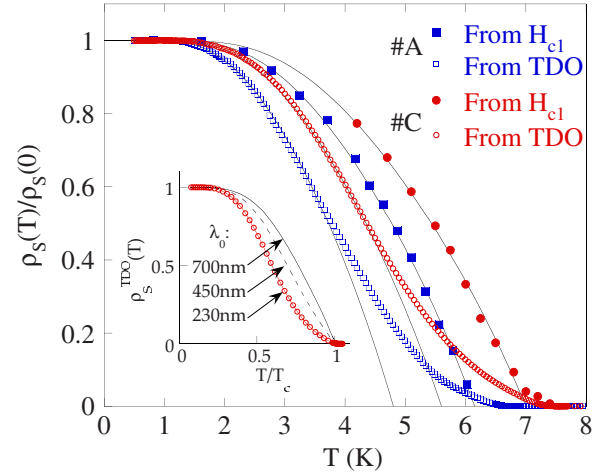


FIG. 3. (Color online) Normalized superfluid density deduced from H_{c1} measurements (full symbols) and TDO measurements with $\lambda_0 = 230$ nm (open symbols) for samples A (squares) and C (circles). The solid lines are the fit for a superconducting gap $\Delta = 2 k_B T_c$ with $T_c = 4.8, 5.6, 6.2,$ and 7 K (see text). Inset: influence of the λ_0 value used to deduce ρ_S from TDO measurements.

played in Fig. 3 for samples A (squares) and C (circles). The two techniques lead to strikingly different temperature dependence for the superfluid density. For an isotropic superconducting gap, the BCS superfluid density $\rho_S(T)$ reduced by thermally activated excitations is expected to be given by

$$\rho_S(T) = 1 - \int \frac{\partial f}{\partial E} \frac{E}{\sqrt{E^2 - \Delta^2(T)}}, \quad (1)$$

where f is the Fermi Dirac distribution, E is the energy above the Fermi energy, and $\Delta(T)$ is the value of the superconducting gap at the temperature T . As shown in Fig. 3 (solid lines) very good fits to the ρ_S^{Hc1} data are obtained using an alpha model in which the temperature dependence of the superconducting gap (normalized to its $T=0$ K value) has been assumed to be equal to the reduced BCS weak-coupling value calculated from the gap equation³³ and taking $\Delta(0) = 2 k_B T_c$. Note that a superconducting gap equal to its weak-coupling theory value [$\Delta(0) = 1.76 k_B T_c$] only leads to a poor fit of the data, confirming the large value of the $\Delta(0)/k_B T_c$ ratio previously obtained by bulk probes such as specific-heat measurements.

On the other hand, ρ_S^{TDO} displays a strong downward curvature at low temperature followed by a clear upward curvature as the superfluid density drops below 0.5 [i.e., for $\lambda(T) > 1.4\lambda_0$]. As pointed out above one has to determine the R/λ_0 ratio in order to deduce ρ_S^{TDO} from the $\delta f/\Delta f_0$ data. The R value has been calculated from the aspect ratio using the formula introduced by Prozorov.²⁸ The validity of this procedure has been checked on Pb samples. Moreover, different ac magnetic field orientations on the same single crystal of MgCNi₃ (but different R) show the same quantitative temperature dependence of $\lambda(T)$, consistently with an isotropic cubic system.

A possible explanation would hence be an underestimation of λ_0 . The influence of λ_0 is displayed in the inset of

Fig. 3. As shown taking $\lambda_0 \approx 700$ nm instead of 230 nm leads to a temperature dependence for ρ_S^{TDO} similar to the one obtained for ρ_S^{Hc1} . This value is however well above our error bars on λ_0 and would correspond to $\mu_0 H_{c1}(0) \sim 15$ G, i.e., even smaller than our first penetration field values (~ 55 G). Note that strong bulk pinning could lead to an overestimation of H_p if measured in the center of the sample (see, for instance, Ref. 34), but we checked that very similar H_p values are obtained for several probe positions by placing the sample on an array of 11 miniature ($10 \times 10 \mu\text{m}^2$) probes: as shown in the left inset of Fig. 2, the field distribution clearly presents the V-shape profile characteristic of a strong bulk pinning. Even though those profiles confirm the good homogeneity of the sample, one can not exclude the presence of a strong disorder at the surface of the samples leading to a surface penetration field much larger than the bulk value. However, the $\lambda_0 = 700$ nm value would require an extremely small mean free path (~ 1 nm, see discussion above). A possible difference between the mixed state and Meissner state penetration depth values associated either to a Doppler shift induced by the supercurrents on the excitation spectra^{35,36} or to a strong field dependence of λ in the mixed state (see, for instance, Ref. 37) due to multiband effects can be excluded in our isotropic fully gapped system.

Another explanation could be a difference between bulk and surface critical temperatures. Indeed, at low-temperature TDO measurements only probe the sample on a typical depth in the order of $\lambda_0 \sim 0.2 \mu\text{m}$, i.e., roughly 0.4% of the total volume (for a volume to surface ratio of $50 \mu\text{m}$). In the presence of a weak-coupling superconducting gap, this volume only increases to about 20% of the sample volume for $T \rightarrow T_c/2$ and the bulk of the sample is only probed close to T_c as the magnetic penetration depth finally diverges for T

$\rightarrow T_c$. On the other hand, the Hall probe has been placed close to the center of the sample in the HPM measurements and is hence sensitive to the bulk of the sample. In the case of MgCNi_3 , it is known that the critical temperature has a surprising high sensitivity to a very small change in the C or Ni stoichiometry^{4,20} and also surface stress.^{14,38} Assuming that the critical temperature of the surface is 20% smaller than the bulk value, very good fit to the data could be obtained for ρ_S^{TDO} using Eq. (1) for $T < \frac{3}{4}T_c$ [still taking $\Delta(0) = 2 k_B T_c$, see solid lines in Fig. 3]. Note that a large dispersion of the T_c values in powder might explain the anomalous temperature dependence observed in previous λ measurements. Clear deviations from the standard BCS theory [Eq. (1)] have been observed in systems such as MgB_2 (Ref. 39) or more recently in pnictides,⁴⁰ but in our case those deviations in ρ_S^{TDO} are due to surface inhomogeneities (disorder and/or T_c) and our measurements emphasize the importance of coupling complementary experimental probes in order to unambiguously address this issue.

To conclude, we have shown that the temperature dependence of the magnetic penetration depth is exponential in MgCNi_3 single crystals signaling the presence of a fully open superconducting gap. A drastically different behavior has systematically been observed between the superfluid density extracted from the lower critical field and TDO measurements performed on the same sample, which are most probably due to surface disorder and/or a depletion of 20% of the critical temperature at the surface.

We are most obliged to V. Mosser of ITRON, Montrouge, for the development of the Hall sensors used in this Rapid Communication. This work was partially supported by the Slovak R & D Agency under Contracts No. VVCE-0058-07, No. APVV-0346-07, and No. LPP-0101-06.

¹D. Aoki *et al.*, Nature (London) **413**, 613 (2001).

²S. S. Saxena *et al.*, Nature (London) **406**, 587 (2000).

³D. J. Singh and M. H. Du, Phys. Rev. Lett. **100**, 237003 (2008).

⁴T. He *et al.*, Nature (London) **411**, 54 (2001).

⁵S. B. Dugdale and T. Jarlborg, Phys. Rev. B **64**, 100508(R) (2001).

⁶H. Rosner *et al.*, Phys. Rev. Lett. **88**, 027001 (2001).

⁷D. J. Singh and I. I. Mazin, Phys. Rev. B **64**, 140507(R) (2001).

⁸P. M. Singer *et al.*, Phys. Rev. Lett. **87**, 257601 (2001).

⁹L. Shan *et al.*, Phys. Rev. B **71**, 144516 (2005).

¹⁰I. I. Mazin *et al.*, Phys. Rev. Lett. **101**, 057003 (2008).

¹¹A. Y. Ignatov, S. Y. Savrasov, and T. A. Tyson, Phys. Rev. B **68**, 220504(R) (2003).

¹²R. Heid *et al.*, Phys. Rev. B **69**, 092511 (2004).

¹³A. Wälte *et al.*, Phys. Rev. B **70**, 174503 (2004).

¹⁴A. Wälte *et al.*, Phys. Rev. B **72**, 100503(R) (2005).

¹⁵T. Klimczuk and R. J. Cava, Phys. Rev. B **70**, 212514 (2004).

¹⁶O. V. Dolgov *et al.*, Phys. Rev. Lett. **95**, 257003 (2005).

¹⁷R. Prozorov, A. Snezhko, T. He, and R. J. Cava, Phys. Rev. B **68**, 180502(R) (2003).

¹⁸J.-Y. Lin *et al.*, Phys. Rev. B **67**, 052501 (2003).

¹⁹L. Shan *et al.*, Phys. Rev. B **68**, 024523 (2003).

²⁰H.-S. Lee *et al.*, Adv. Mater. **19**, 1807 (2007).

²¹J. Kacmarcik *et al.*, Acta Phys. Pol. A **113**, 363 (2008).

²²C. T. Van Degrift, Rev. Sci. Instrum. **46**, 599 (1975).

²³A. Carrington *et al.*, Phys. Rev. Lett. **83**, 4172 (1999).

²⁴R. Prozorov *et al.*, Appl. Phys. Lett. **77**, 4202 (2000).

²⁵J. D. Fletcher *et al.*, Phys. Rev. Lett. **98**, 057003 (2007).

²⁶G. Kinoda *et al.*, Jpn. J. Appl. Phys., Part 2 **40**, L1365 (2001).

²⁷L. Shan *et al.*, Phys. Rev. B **68**, 144510 (2003).

²⁸R. Prozorov, R. W. Giannetta, A. Carrington, and F. M. Araujo-Moreira, Phys. Rev. B **62**, 115 (2000).

²⁹E. H. Brandt, Phys. Rev. B **59**, 3369 (1999).

³⁰E. Zeldov *et al.*, Phys. Rev. Lett. **73**, 1428 (1994).

³¹G. MacDougall *et al.*, Physica B **374-375**, 263 (2006).

³²X. F. Lu *et al.*, Phys. Rev. B **71**, 174511 (2005).

³³H. Padamsee, J. Neighbor, and C. Shiffman, J. Low Temp. Phys. **12**, 387 (1973).

³⁴R. Okazaki *et al.*, Phys. Rev. B **79**, 064520 (2009).

³⁵S. K. Yip and J. A. Sauls, Phys. Rev. Lett. **69**, 2264 (1992).

³⁶D. Xu, S. K. Yip, and J. A. Sauls, Phys. Rev. B **51**, 16233 (1995).

³⁷T. Klein *et al.*, Phys. Rev. B **73**, 184513 (2006).

³⁸M. Uehara *et al.*, Physica C **440**, 6 (2006).

³⁹A. A. Golubov, A. Brinkman, O. V. Dolgov, J. Kortus, and O. Jepsen, Phys. Rev. B **66**, 054524 (2002).

⁴⁰R. T. Gordon *et al.*, Phys. Rev. Lett. **102**, 127004 (2009).